Supplementary material

Table S1. Chemical compositions of simulated CSSs.

№	Ni, at.%	Fe, at.%	Cr, at.%
1	100	0	0
2	90	0	10
3	80	0	20
4	60	0	40
5	50	0	50
6	90	10	0
7	80	10	10
8	70	10	20
9	50	10	40
10	40	10	50
11	80	20	0
12	70	20	10
13	60	20	20
14	40	20	40
15	33.4	33.3	33.3
16	60	40	0
17	50	40	10
18	40	40	20
19	50	50	0
20	40	50	10

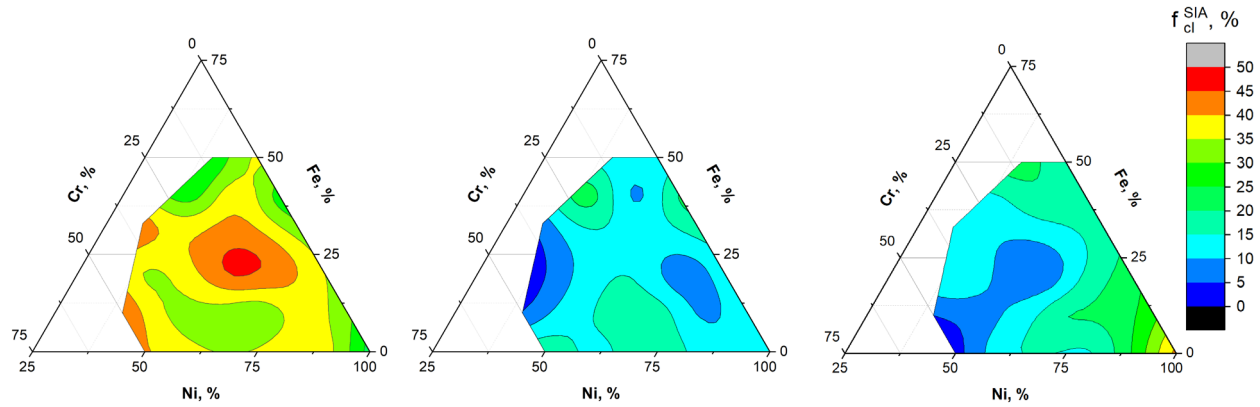

Fig. S1. (Color online) The fraction of SIAs forming clusters of sizes 2–11 (a), 12–21 (b) and more than 21 defects (c) 20 ps after generation of atomic displacement cascade in samples of different chemical compositions.

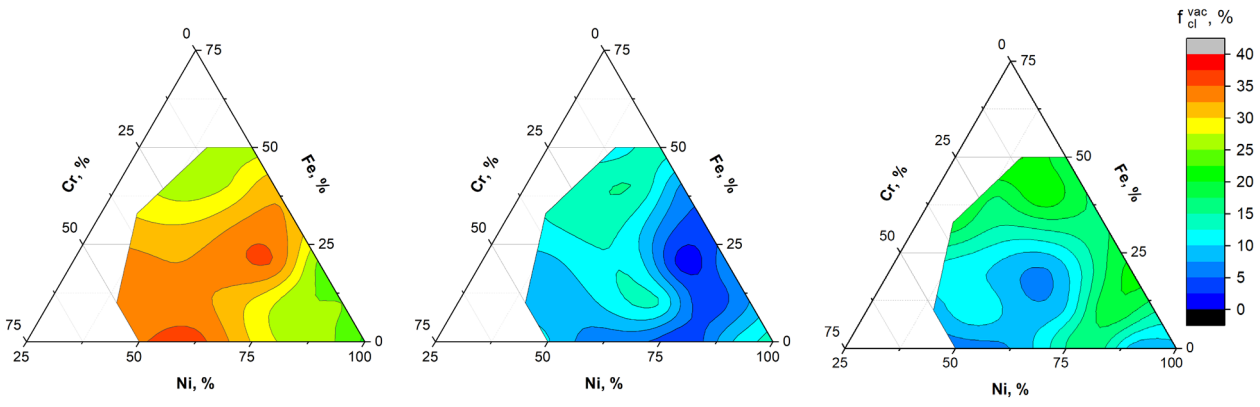

Fig. S2. (Color online) The fraction of vacancies forming clusters of sizes 2–11 (a), 12–21 (b) and more than 21 defects (c) 20 ps after generation of atomic displacement cascade in samples of different chemical compositions.

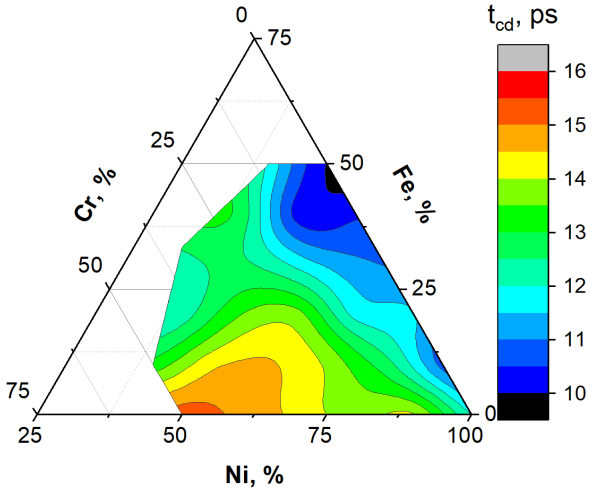

Fig. S3. (Color online) Time of cooling down for single cascades in samples of different chemical compositions.

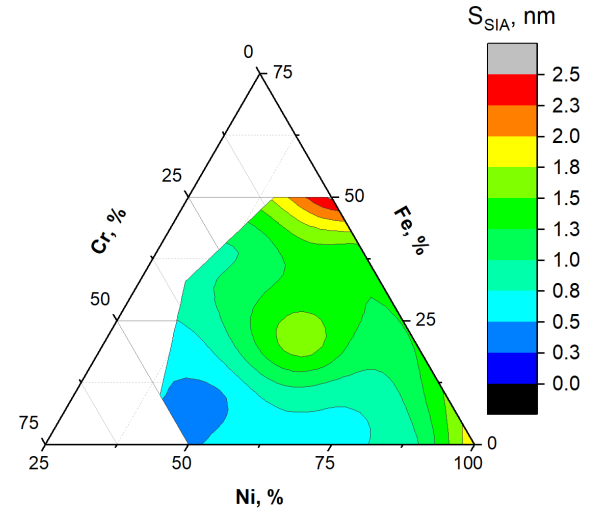

Fig. S4. (Color online) Distance covered by a single SIA for 0.1 ns in samples of different chemical compositions.

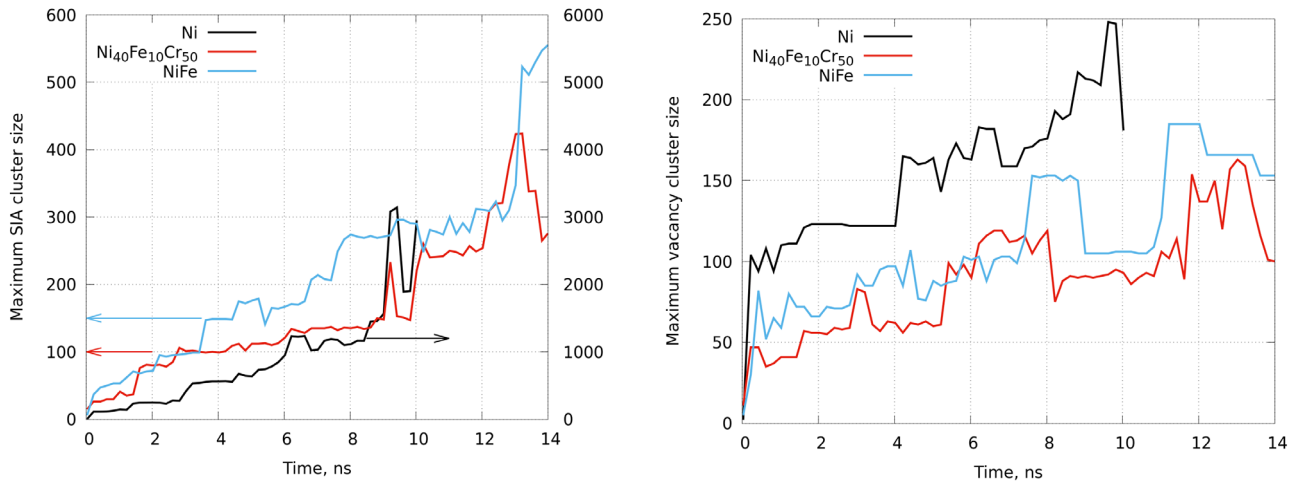

a b

Fig. S5. (Color online) Size of the largest SIA (a) and vacancy (b) clusters versus time for different chemical compositions under prolonged irradiation.

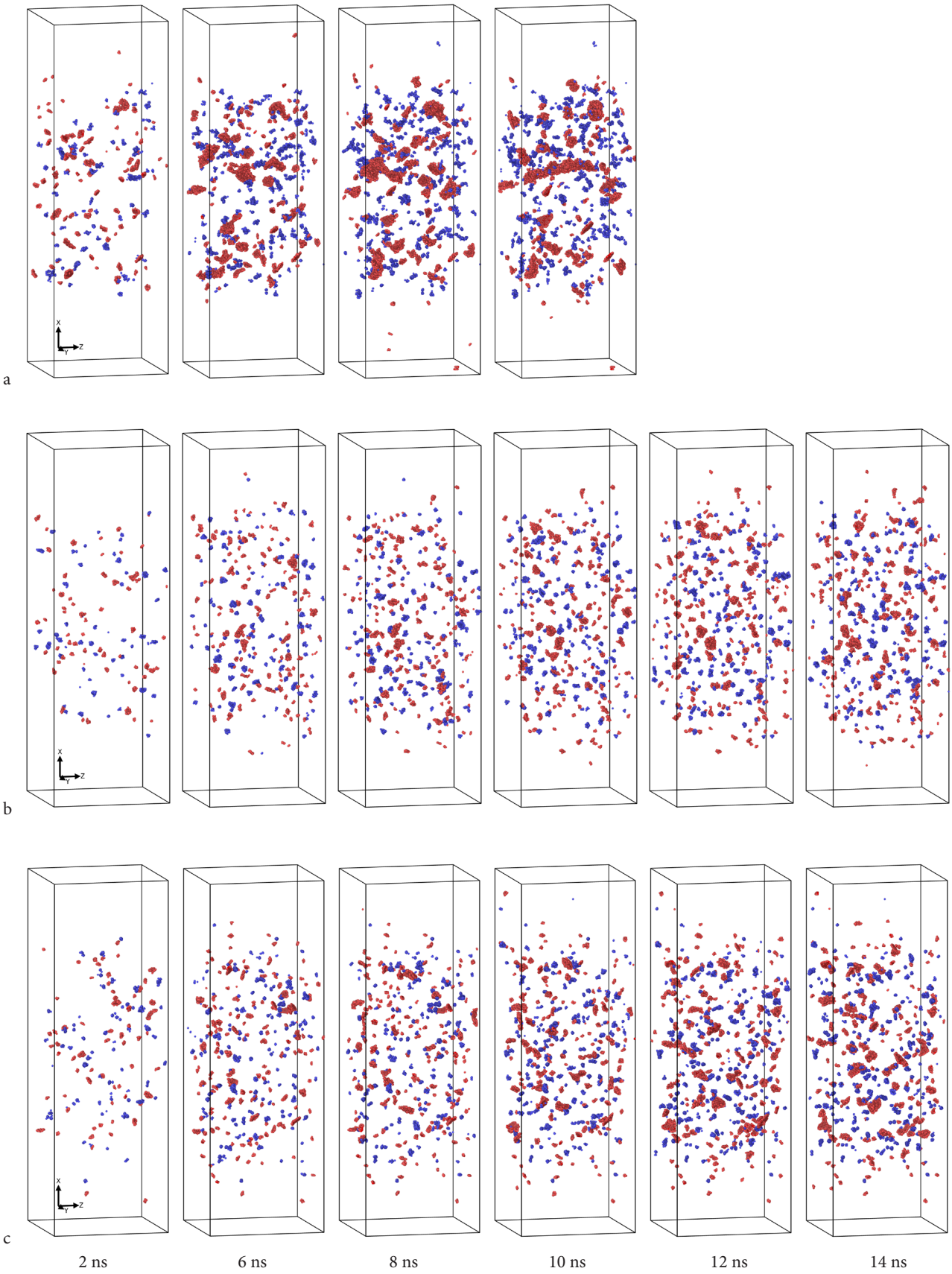

Fig. S6. (Color online) Spatial distribution of vacancies (blue) and SIAs (red) in Ni (a), $Ni_{40}Fe_{10}Cr_{50}$ (b) and NiFe (c) at different times under prolonged irradiation. Defects in clusters with size smaller than 10 are not shown.

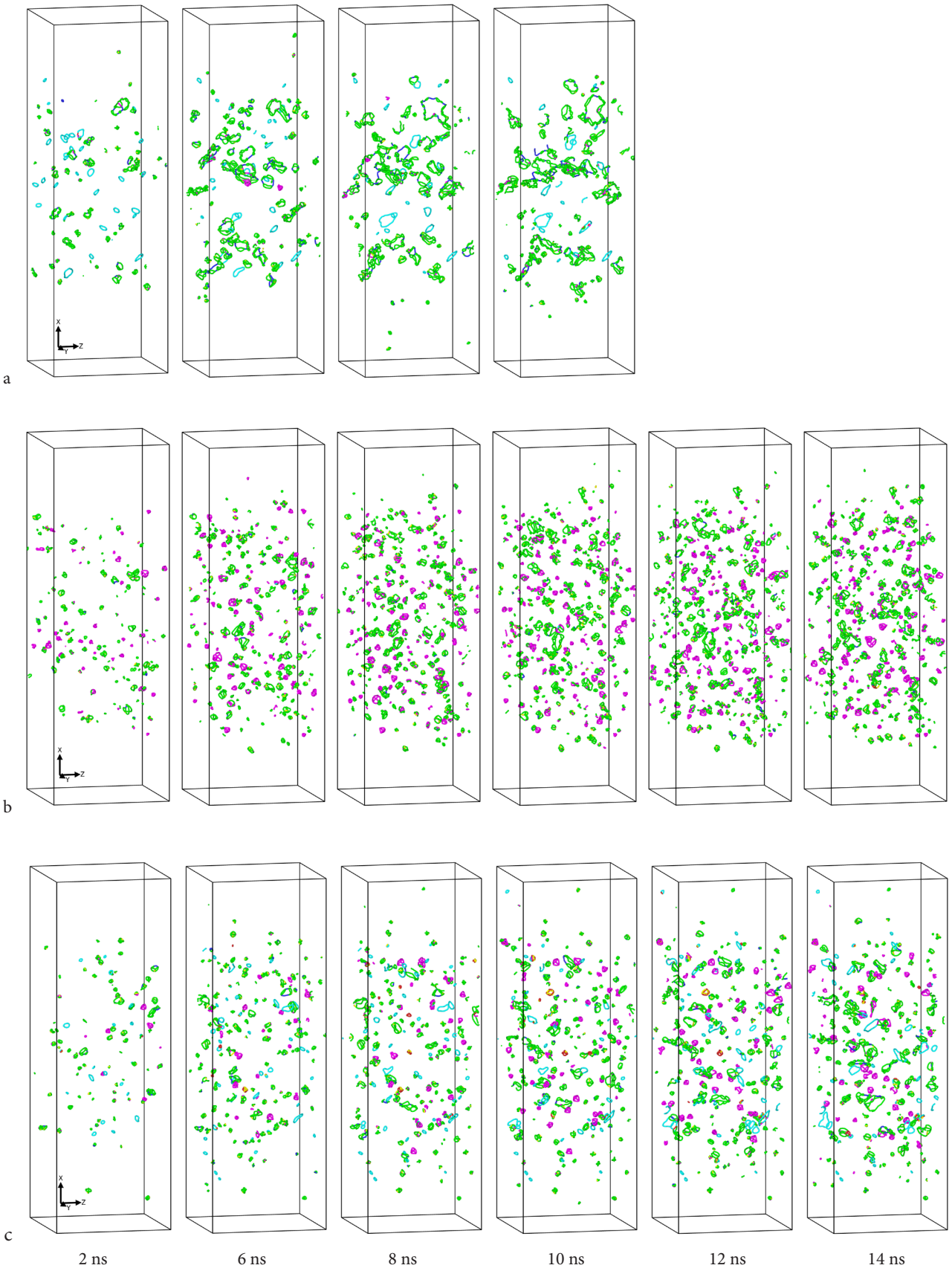

Fig. S7. (Color online) Dislocation structure in Ni (a), $Ni_{40}Fe_{10}Cr_{50}$ (b) and NiFe (c) at different times under prolonged irradiation. Green lines — 1/6<112> dislocations, magenta — 1/6<110>, cyan — 1/3<111>, blue — 1/2<110>.